Supporting Information

β-Cyclodextrin Included Coumarin Derivatives as Selective Fluorescent Sensors for Cu^{2+} Ion in HeLa Cells

Raihana Imran Khan[a] and Kasi Pitchumani[ab]*

[a]School of Chemistry, Madurai Kamaraj University, Madurai 625 021.
[b]*Center for Green Chemistry Processes, School of Chemistry, Madurai Kamaraj University, Madurai, India.

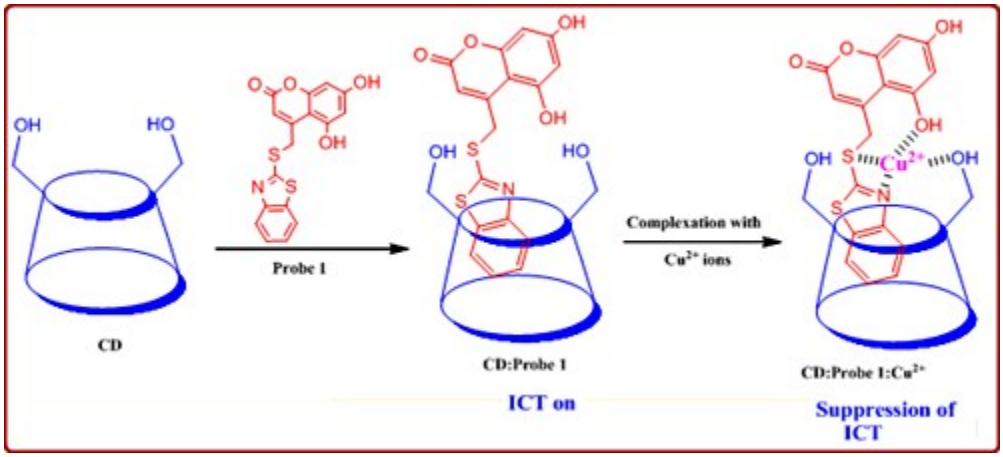

Contents: **Page No.**

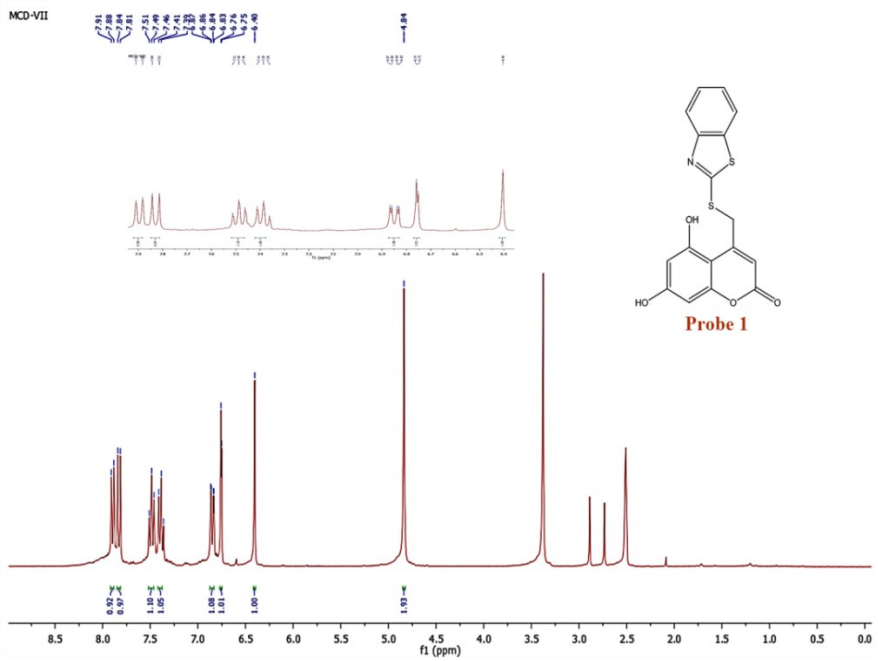

Fig. S1 ^{1}H-NMR (300 MHz, DMSO-d_6) spectrum of 4-((benzo[*d*]thiazol-2-ylthio)methyl)- 5, 7-hydroxy-2H-chromen-2-one **1**. ^{1}H NMR (300 MHz, DMSO-d_6) δ 7.91 (s, 1H), 7.83 (d, J = 8.7 Hz, 1H), 7.50 (d, J = 7.5 Hz, 1H), 7.40 (d, J = 7.9 Hz, 1H), 6.85 (dd, J = 8.7, 2.2 Hz, 1H), 6.76 (d, J = 2.2 Hz, 1H), 6.40 (s, 1H), 4.84 (s, 2H).

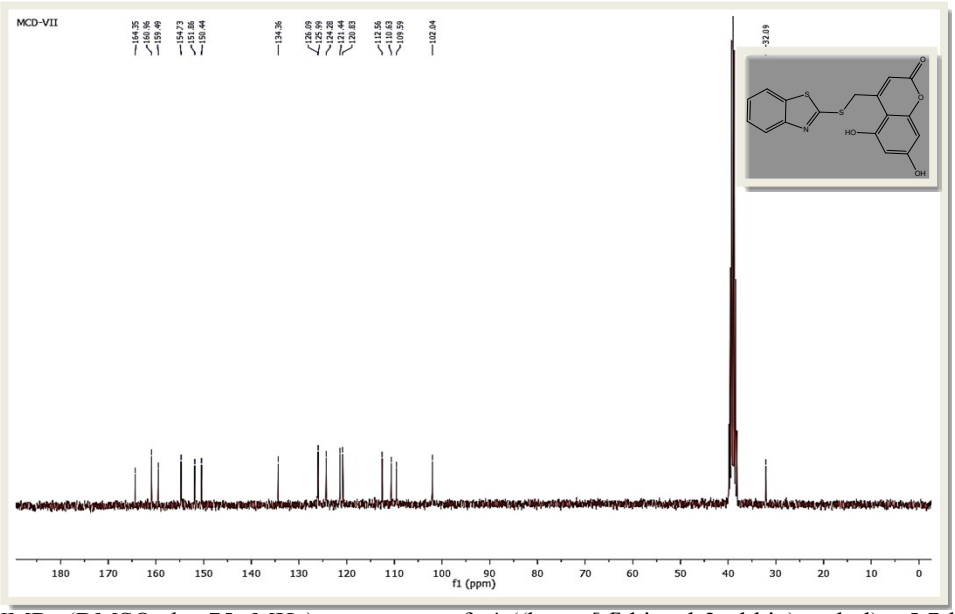

Fig. S2 ^{13}C-NMR (DMSO-d_6, 75 MHz) spectrum of 4-((benzo[*d*]thiazol-2-ylthio)methyl)- 5,7-hydroxy-2H-chromen-2-one **1.** ^{13}C NMR (DMSO-d_6, 75 MHz) δ/ppm 31.9, 101.3, 109.6, 110.8, 112.5, 120.4, 121.6, 124.2, 125.0, 125.7, 134.4, 151.4, 154,6, 159.3, and 160.4.

.

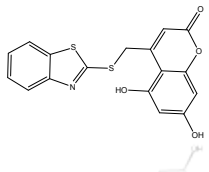

Exact Mass 357.23
Observed Mass 395.08
(M+K)

Fig. S3 ESI-Mass spectrum of 4-((benzo[*d*]thiazol-2-ylthio)methyl)- 5, 7-hydroxy-2H-chromen-2-one **1**. ESI MS peak at m/z 395.08 $[M+K]^+$ value is observed for 1.

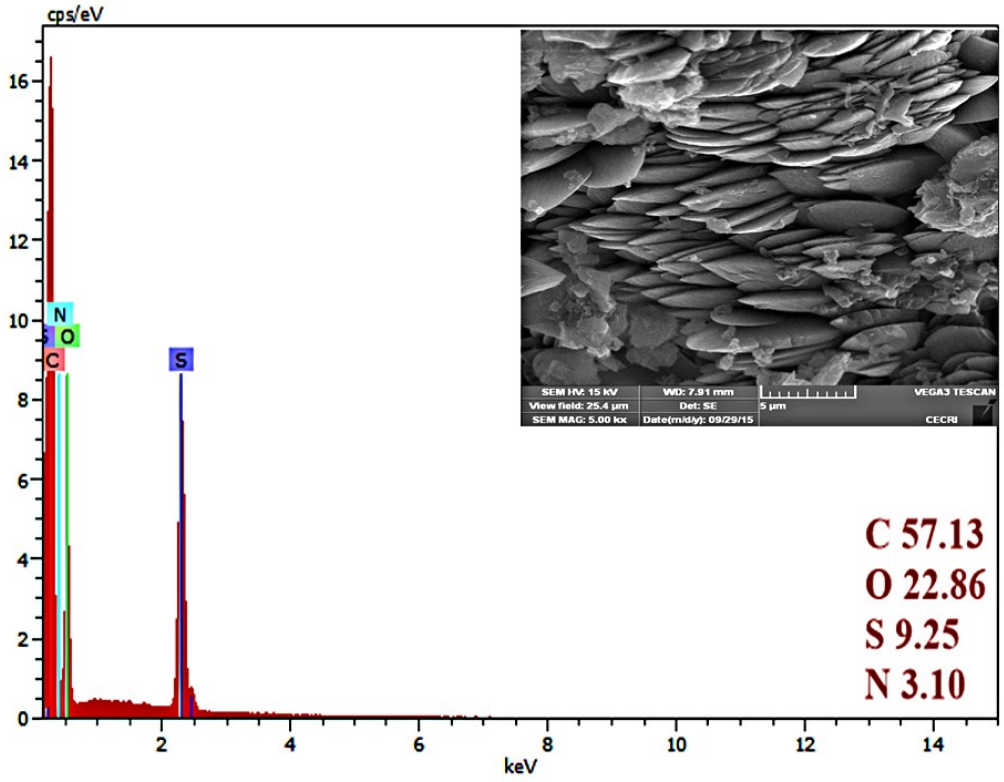

Fig. S 4 SEM-EDX spectrum of 4-((benzo[*d*]thiazol-2-ylthio)methyl)- 5, 7-hydroxy-2H-chromen-2-one 1. Anal. found: C, 57.13; O, 22.86; S, 13.25; and N, 3.10 values are observed.

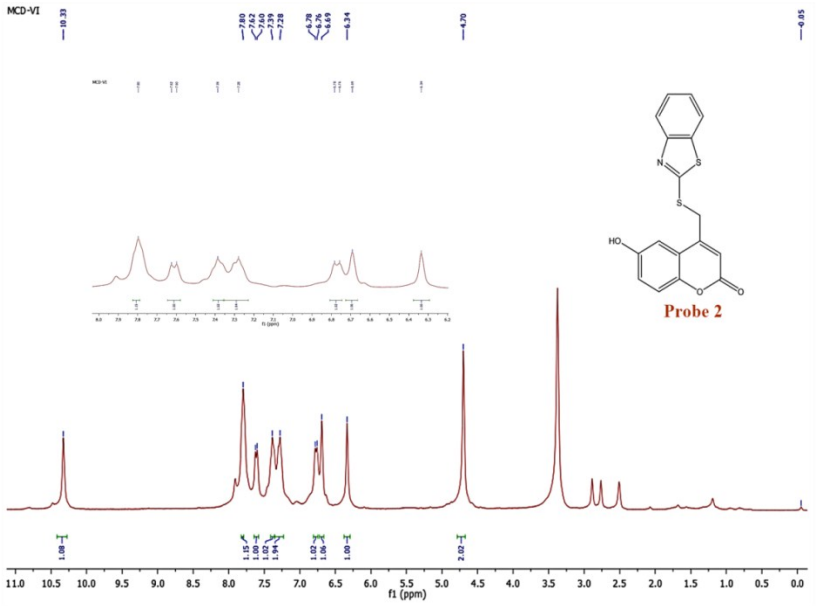

Fig. S5 ^{1}H-NMR (300 MHz, DMSO-d_6) spectrum of 4-((benzo[*d*]thiazol-2-ylthio)methyl)-5-hydroxy-2H-chromen-2-one 2. ^{1}H NMR (300 MHz, DMSO-d_6) δ 10.33 (s, 1H), 7.80 (s, 1H), 7.61 (d, J = 7.9 Hz, 1H), 7.39 (s, 1H), 7.28 (s, 2H), 6.77 (d, J = 7.6 Hz, 1H), 6.69 (s, 1H), 6.34 (s, 1H), 4.70 (s, 2H).

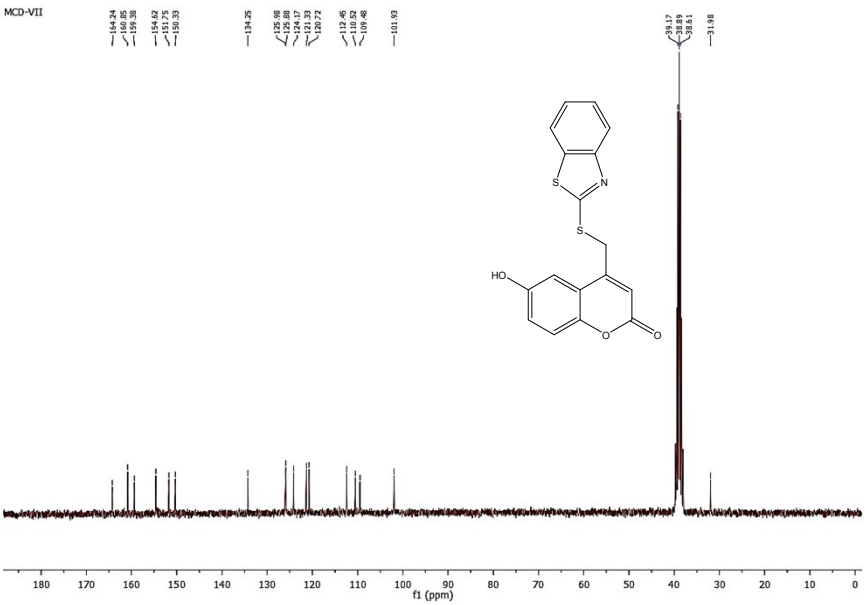

Fig. S6 ^{13}C-NMR (DMSO-d_6, 75 MHz) spectrum of 4-((benzo[*d*]thiazol-2-ylthio)methyl)-5-hydroxy-2H-chromen-2-one **2.** ^{13}C NMR (DMSO-d_6, 75 MHz) δ/ppm 31.98, 101.93, 109.48, 110.52, 112.45, 120.72, 121.33, 124.17, 125.88, 125.98, 134.25, 150.33, 151.75, 154.62, 159.38, 160.85, and 164.24.

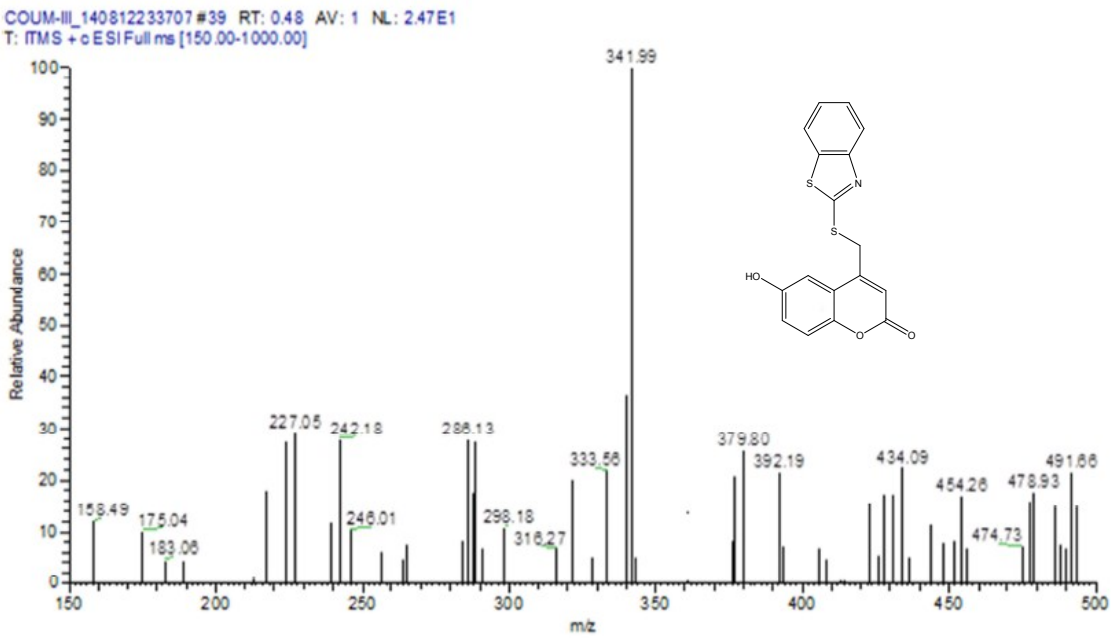

Fig. S7 ESI-Mass spectrum of 4-((benzo[*d*]thiazol-2-ylthio)methyl)- 5, 7-hydroxy-2H-chromen-2-one **2.** ESI MS peak at m/z 341.99 $[M+H]^+$ value is observed.

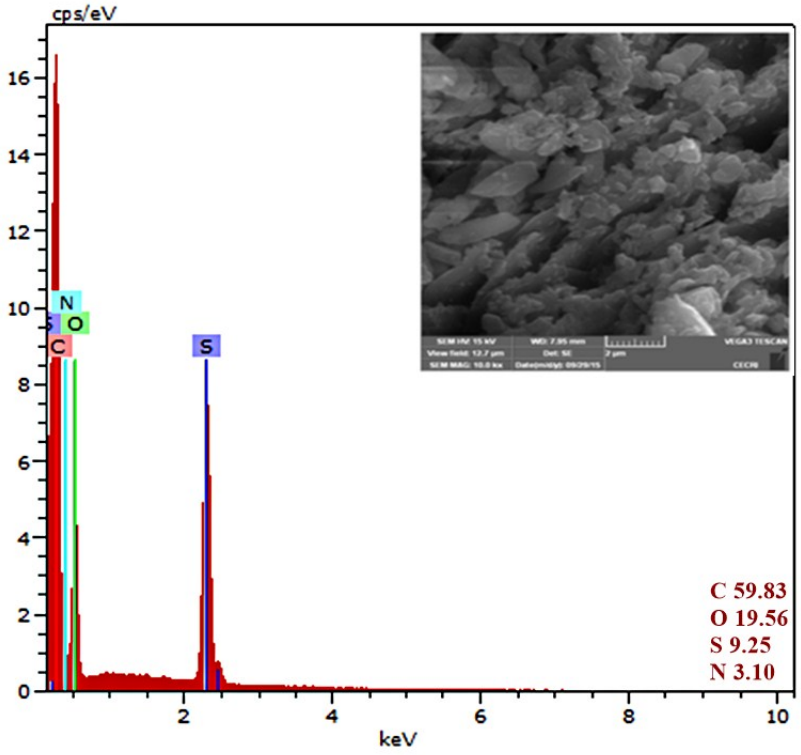

Fig. S 8 SEM-EDX spectrum of 4-((benzo[*d*]thiazol-2-ylthio)methyl)-5-hydroxy-2H-chromen-2-one **2.** Anal. found: C, 59.83; O, 19.56; S, 13.25; and N, 3.10 values are observed.

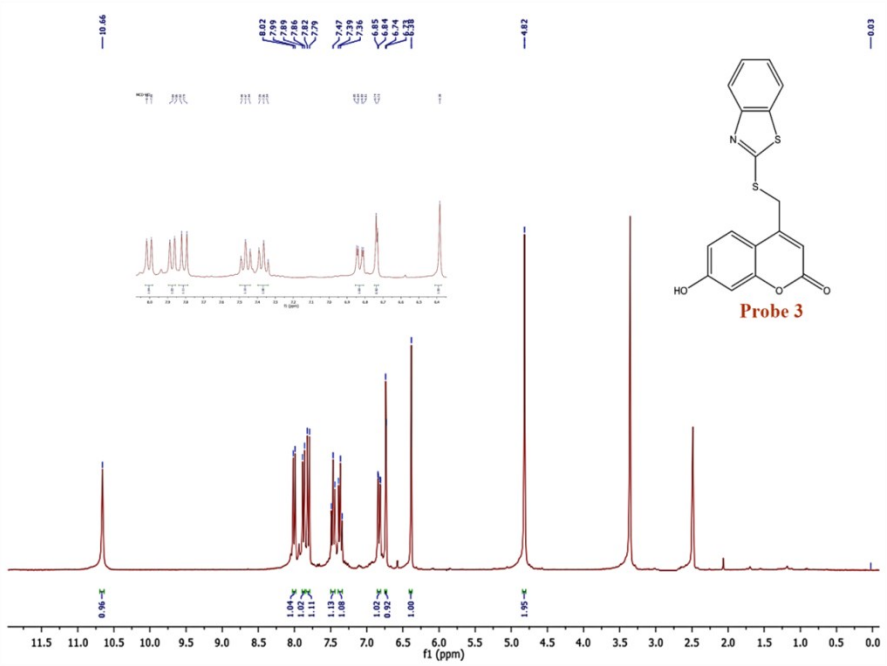

Fig. S9 ^{1}H-NMR (300 MHz, DMSO-d_6) spectrum of 4-((benzo[*d*]thiazol-2-ylthio)methyl)-7-hydroxy-2H-chromen-2-one **3.** ^{1}H NMR (300 MHz, DMSO-d_6) δ 10.66 (s, 1H), 8.00 (d, J = 7.8 Hz, 1H), 7.87 (d, J = 8.1 Hz, 1H), 7.81 (d, J = 8.7 Hz, 1H), 7.47 (t, J = 7.6 Hz, 1H), 7.38 (d, J = 7.9 Hz, 1H), 6.83 (dd, J = 8.7, 2.2 Hz, 1H), 6.73 (d, J = 2.2 Hz, 1H), 6.38 (s, 1H), 4.82 (s, 2H).

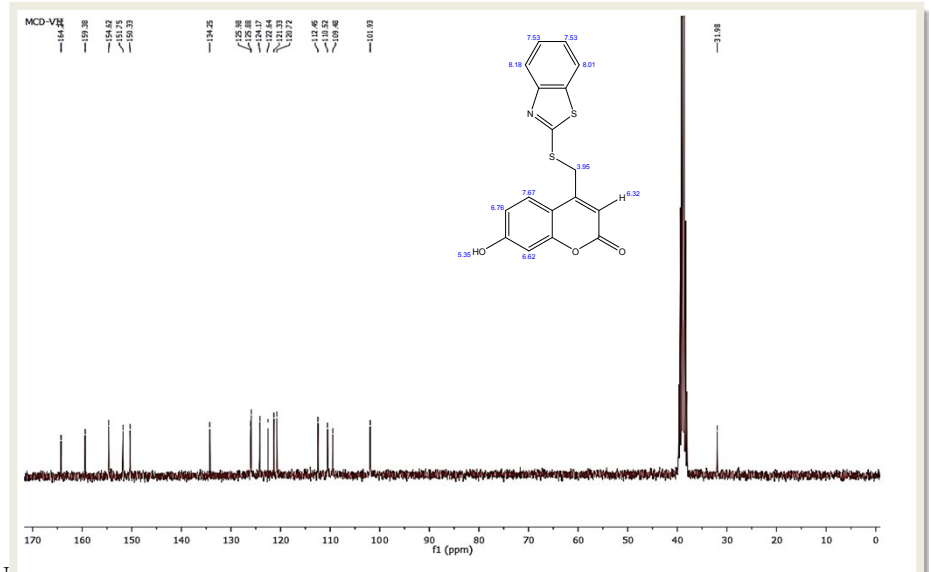

Fig. S10 ^{13}C-N[illegible] spectrum of 4-((benzo[d]thiazol-2-ylthio)methyl)-7-hydroxy-2H-chromen-2-one **3**. ^{13}C NMR (DMSO-d_6, 75 MHz) δ/ppm 31.98, 101.93, 109.48, 110.52, 112.45, 120.72, 121.33, 122.64, 124.67, 125.88, 125.98, 134.25, 150.33, 151.75, 154.64, 159.38, and 164.12.

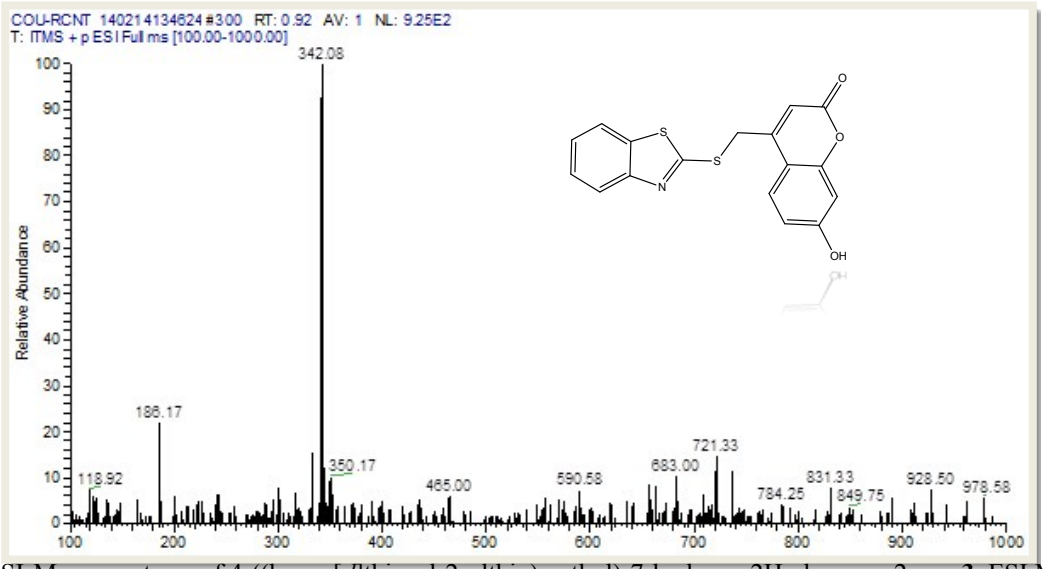

Fig. S11 ESI-Mass spectrum of 4-((benzo[*d*]thiazol-2-ylthio)methyl)-7-hydroxy-2H-chromen-2-one **3.** ESI MS peak at m/z 342.08 $[M+H]^+$ value is observed.

Absorption and Emission Spectra for CD:1, 2 and 3:

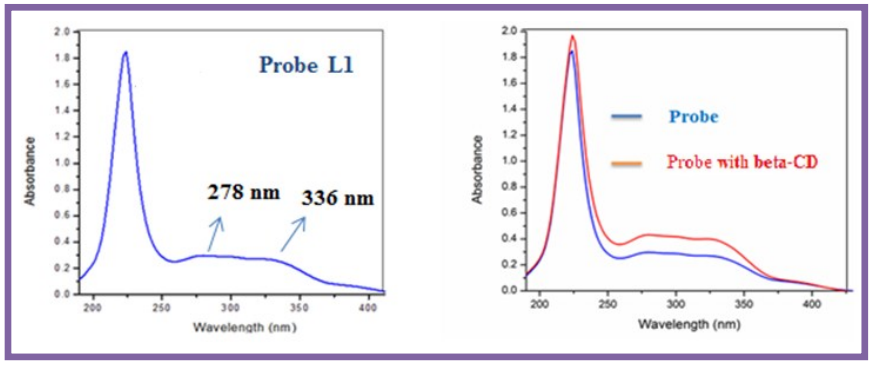

Fig. S12 UV-Vis. absorption spectra for **1** and absorption spectra for inclusion complex of **1** with *β*-cyclodextrin (1:1 equ) in aqueous solution (6×10^{-6} mol L^{-1}).

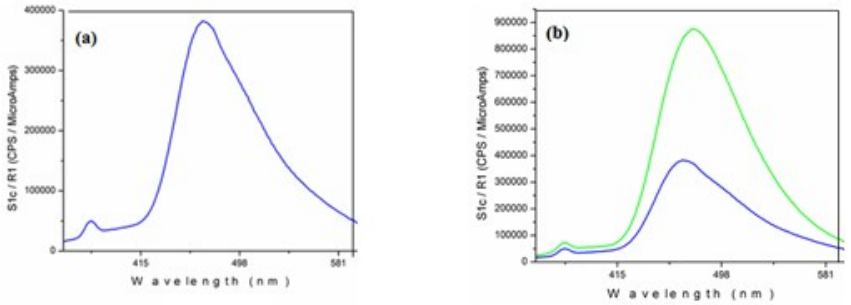

Fig. S13 (a) Fluorescence emission spectra of (a) **1** 4-((benzo[d]thiazol-2-ylthio)methyl)-7-hydroxy-2H-chromen-2-one (6.0×10^{-6}mol $L^{-1}\lambda_{ex}$ = 350 nm, λ_{em} = 465 nm) and (b) emission spectra of **1** and **CD:1** (6.0×10^{-6}mol L^{-1} λ_{ex} = 350 nm, λ_{em} = 475 nm)**.**

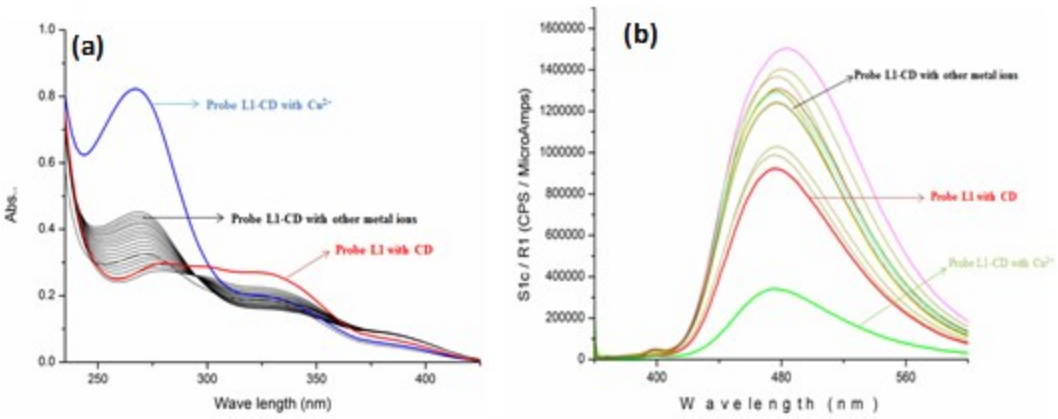

Figure S14. (a) Absorption spectra and (b) fluorescence emission spectra of CD:1 (20 and 5 μM, respectively) with addition of chloride salts of Cd^{2+}, Ag^{+}, Sr^{2+}, Ba^{2+}, Zn^{2+}, Pb^{2+}, Co^{2+}, Hg^{2+}, Mn^{2+}, Fe^{2+}, Ni^{2+}, Cu^{2+} + Other metals (500 μM, respectively) in aqueous solution with an excitation at 350 nm.

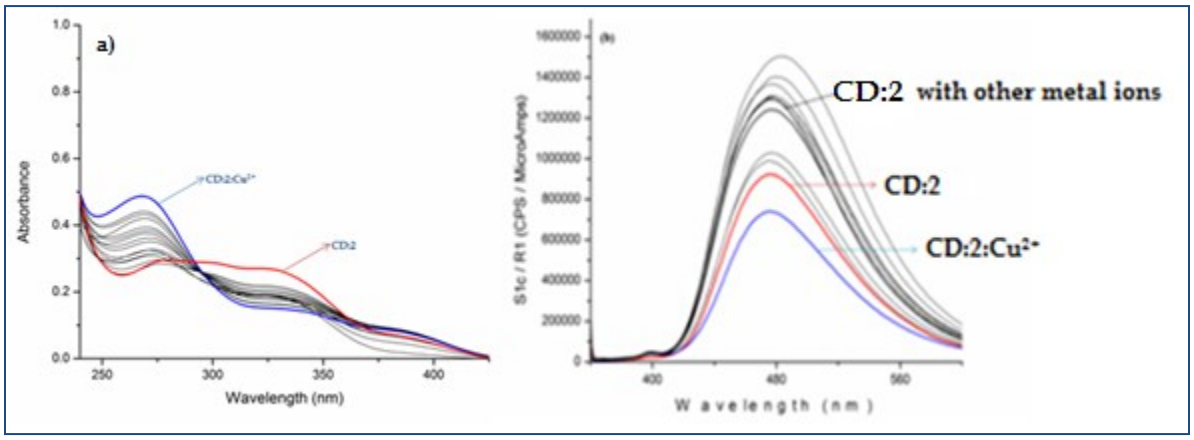

Figure S15. (a) Absorption spectra and (b) fluorescence emission spectra of CD:2 (20 and 5 μM, respectively) with addition of chloride salts of Cd^{2+}, Ag^{+}, Sr^{2+}, Ba^{2+}, Zn^{2+}, Pb^{2+}, Co^{2+}, Hg^{2+}, Mn^{2+}, Fe^{2+}, Ni^{2+}, Cu^{2+} + Other metals (500 μM, respectively) in aqueous solution with an excitation at 350 nm.

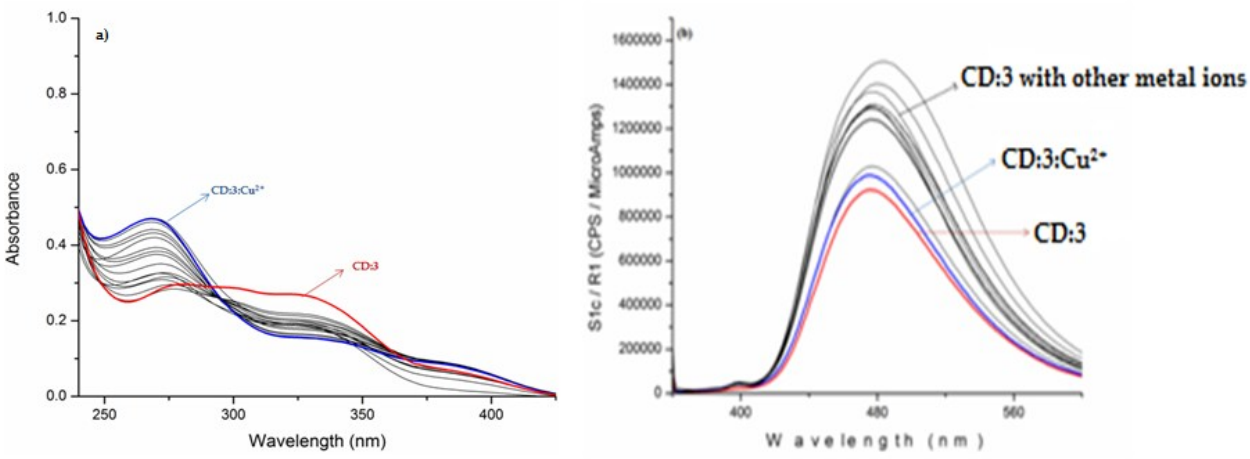

Figure S16. (a) Absorption spectra and (b) fluorescence emission spectra of CD:3 (20 and 5 μM, respectively) with addition of chloride salts of Cd^{2+}, Ag^{+}, Sr^{2+}, Ba^{2+}, Zn^{2+}, Pb^{2+}, Co^{2+}, Hg^{2+}, Mn^{2+}, Fe^{2+}, Ni^{2+}, Cu^{2+} + Other metals (500 μM, respectively) in aqueous solution with an excitation at 350 nm.

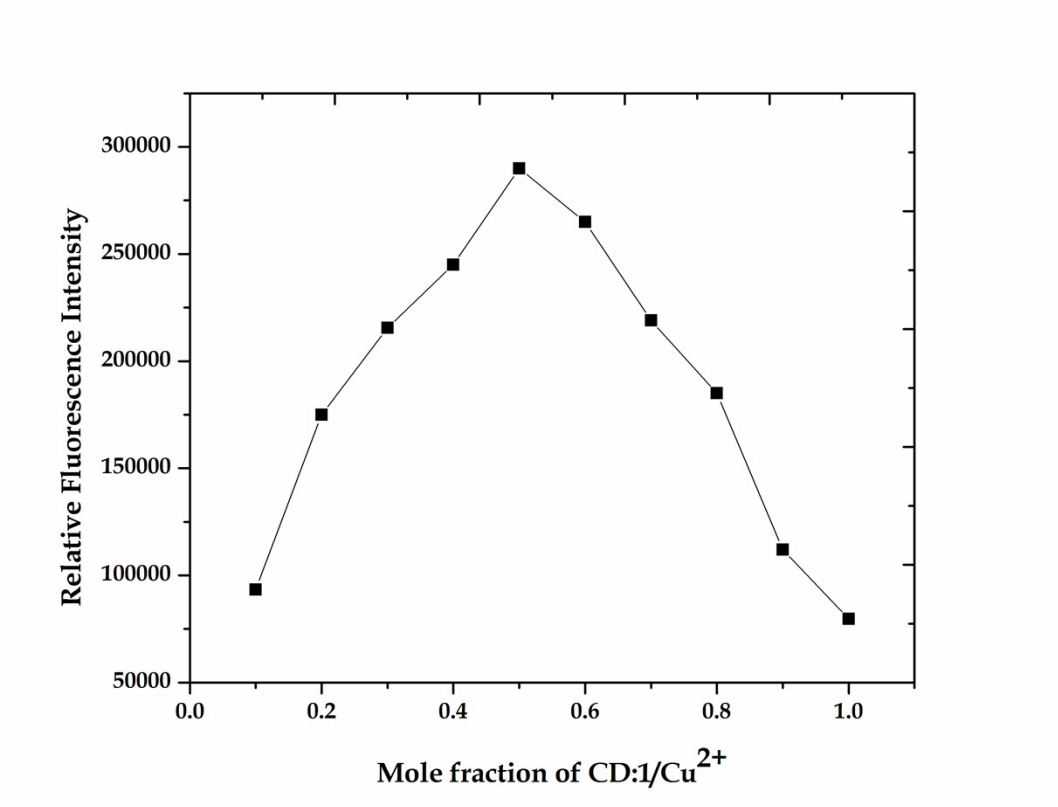

Figure S17. Job's plot diagram between CD:1 and Cu^{2+}

Calculation of Binding constant:

The binding constant K was determined from the plot of the linear regression of

log [(F - F0) / (Fm - F)] vs. log [M] in equation to obtain the intercept as log K and the slope as n.

$$\log \frac{F - F_0}{F_m - F} = \log K + n \log [M]$$

Calculation of Detection limit:

The limit of detection was found using this equation.

$DL = C_L \times C_T$

C_L = Conc. of Ligand; C_T = Conc. of Titrant at which change observed.

Thus; $DL = 6\times10^{-6} \times 0.042\times10^{-5} = 2.52\times10^{-10} = 0.00025\times10^{-7}$

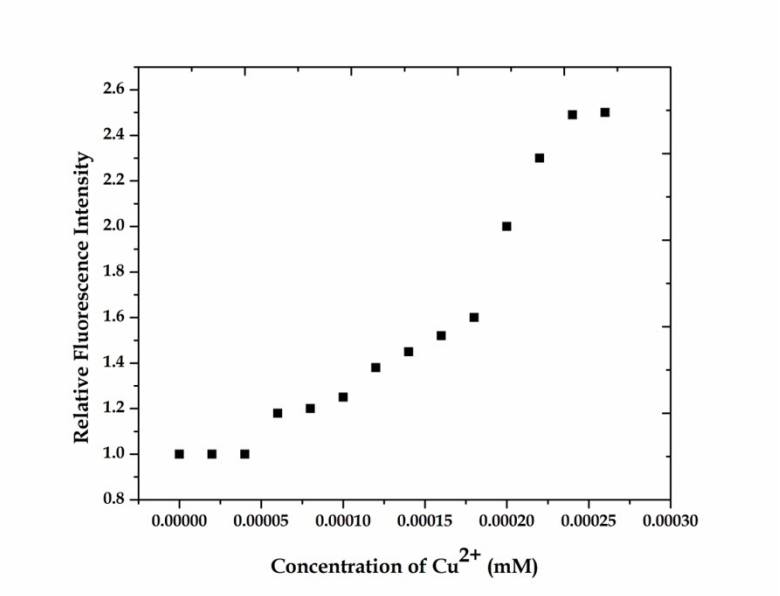

Figure S18. Calculation of Detection limit between CD:1 and Cu^{2+}

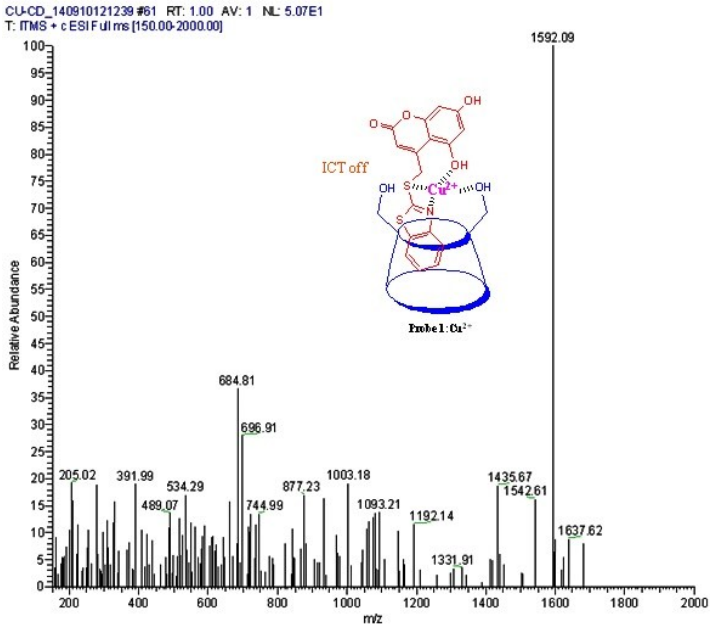

Figure S19. ESI-mass spectrum for inclusion complex of 4-((benzo[*d*]thiazol-2-ylthio)methyl)-7-hydroxy-2H-chromen-2-one in beta-cyclodextrin with Cu^{2+} ion (β-CD:1 + Cu^{2+} ion+ K^+ adduct).

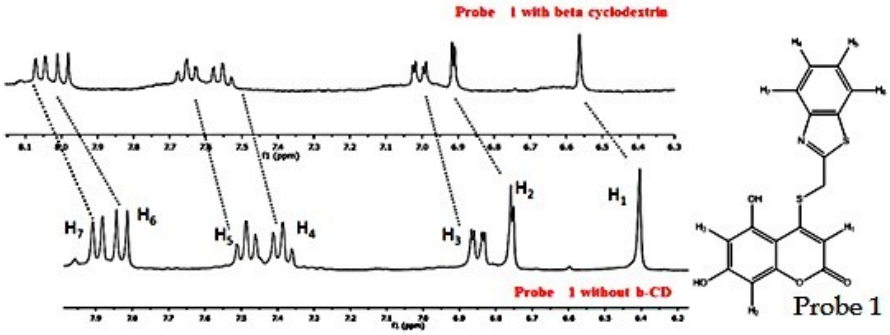

Figure S20. [1]H-NMR spectrum for probe **1** with inclusion of *β*-cyclodextrin and probe **1** without inclusion in β-CD.

Molecular modeling study of 1 with beta-cyclodextrin

Energy minimization studies

Energy minimized geometries of the complexes were obtained using Molecular Mechanics Calculations by INSIGHT II/DISCOVER program.[S1–S4] The initial structures of host and guest molecules were constructed by INSIGHT II/DISCOVER on Silicon Graphics IRIS workstation. We have adapted CVFF force field to express the MM energies of *β*-cyclodextrin (**1**) host, probe and their complexes. Structures were minimized using CVFF force field and RMS derivative 0.001 was achieved in each case. Complexation energies were calculated using the following equation $\Delta E = \Delta E_{Complex} - \Delta E_{Host} - \Delta E_{Guest}$. Figure S16-S21 gives detailed evidence for the probable mode of inclusion of **1**, **2**, and **3** and also the binding energies of both modes.

Table S1. Molecular Modeling studies of **1**with *β*-CD.

Coumarin derivatives	**Mode of Inclusion (Mode A- Primary, Mode B- Secondary sides in β-CD)**	***β*-CD as Host (ΔE^a Kcal.M^{-1})**
1	**Mode A**	**-83.7214**
	Mode B	-75.6233
2	Mode A	-73.6694
	Mode B	-48.8758
3	Mode A	-77.4224
	Mode B	-47.3413

[a]Binding energies of the substrate $\Delta E_{complex} - \Delta E_{host} - \Delta E_{guest}$; each substrate was minimized using AMBER force field. Mode A: inclusion of 1,2 and 3 with primary sides of *β*-CD cavity; Mode B: inclusion of 1, 2 and 3 with secondary sides of *β*-CD cavity.

Table S2: Molecular modeling for 1 with *β*-cyclodextrin favour for thiazolidine part.

Coumarin derivative	**Mode of Inclusion**	***β*-CD as Host (ΔE^a Kcal.M^{-1})**
1	**Mode A**	**-83.4251**
	Mode B	**-75.6233**

[a]Binding energies of the substrate $\boldsymbol{\Delta E_{complex} - \Delta E_{host} - \Delta E_{guest}}$; each substrate was minimized using AMBER force field. **Mode A:** inclusion of thiazolidine part inside the *β*-CD cavity; **Mode B**: inclusion of coumarin part inside the *β*-CD cavity.

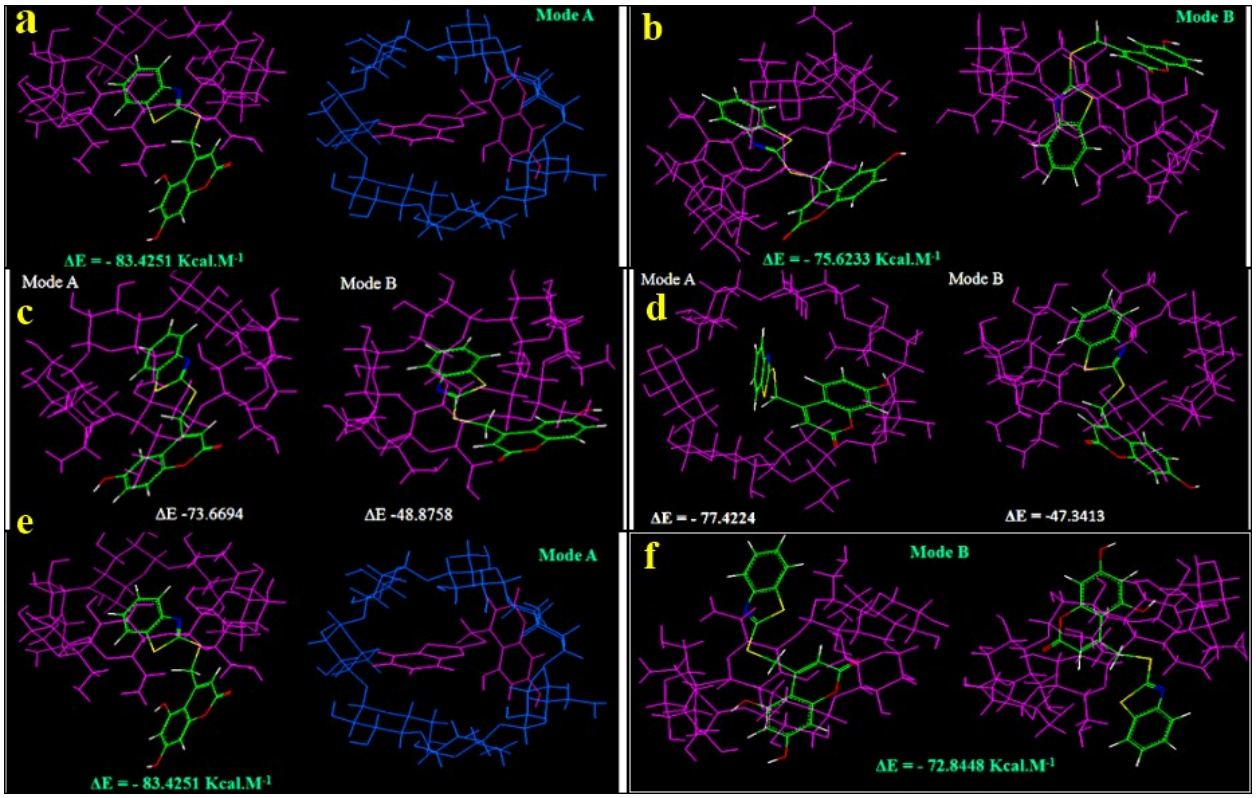

Figure S21: a) CVFF optimized inclusion complex of *β*-cyclodextrin with **1; Mode A:** inclusion of **1** in primary sides of *β*-cyclodextrin. b) CVFF optimized inclusion complex of *β*-cyclodextrin with **1; Mode B**: inclusion of **1** in secondary sides of *β*-cyclodextrin. c) CVFF optimized inclusion complex of *β*-cyclodextrin with **2**; **Mode A**: inclusion of **2** in primary sides of *β*-cyclodextrin; **Mode B**: inclusion of **2** in secondary sides of *β*-cyclodextrin. d) CVFF optimized inclusion complex of *β*-cyclodextrin with **3**; **Mode A:** inclusion of **3** in primary sides of *β*-cyclodextrin; **Mode B**: inclusion of **3** in secondary sides of *β*-cyclodextrin. e) CVFF optimized inclusion complex of *β* -cyclodextrin with **1**; **Mode A**: inclusion of thiazolidine part in *β*-cyclodextrin. f) CVFF optimized inclusion complex of *β* -cyclodextrin with **1**; **Mode B**: inclusion of coumarin part in *β* -cyclodextrin.

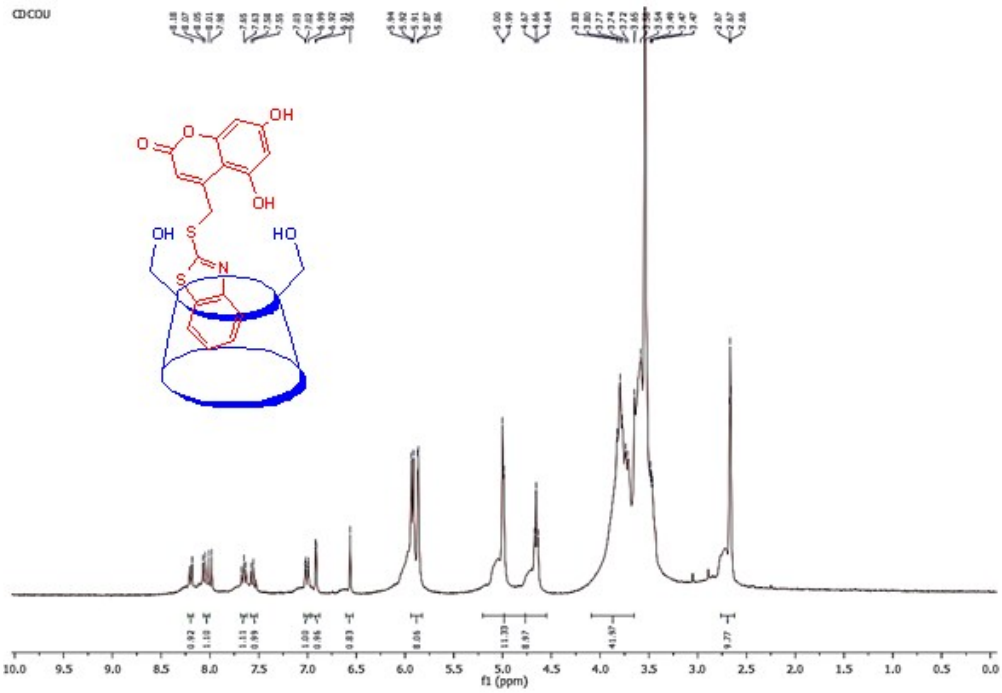

Figure S22 ^{1}H-NMR spectrum for inclusion complex of CD:1 in DMSO-d_6.

NOESY Spectrum of inclusion complex (CD:1) for β-Cyclodextrin and 4-((benzo[*d*]thiazol-2-ylthio)methyl)-5, 7-hydroxy-2H-chromen-2-one(1).

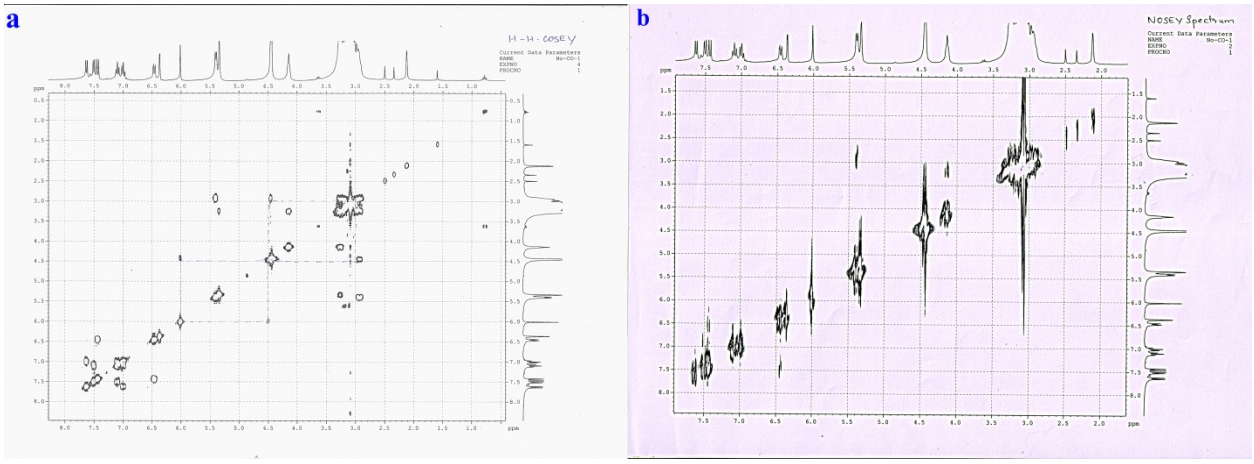

Figure S23 a) H-H COSY Spectrum for inclusion complex of CD:1 in DMSO-d_6. b) NOESY spectrum for inclusion complex of CD:1 in DMSO-d_6.

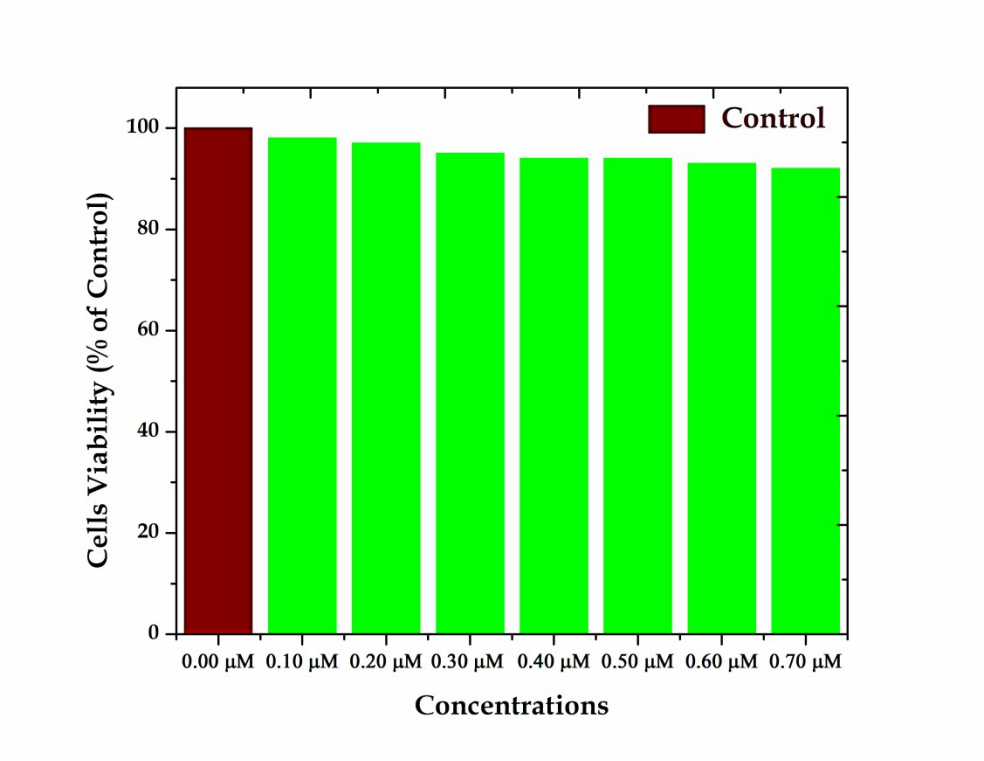

Figure S24 Cell viability values (%) estimated by an MTT assay versus incubation concentrations of CD:1. HeLa cells were cultured in the presence of CD:1 (0–70 mM) at 37 ^{0}C for 24 h

References

S1. P. R. Ashton, R. Koniger, J. F. Stoddart, *J. Org. Chem,* 1996, **61**, 903.

S2. J. I. Choe, K. Kim, S. K. Chang, *Bull. Korean Chem. Soc*, 2000, **21**, 200.

S3. J. I. Choe, S. K. Chang, *Bull. Korean Chem. Soc*, 2002, **23**, 48.

S4. Discover User Guide, *Accelrys*, 2001.